•土木工程•

DOI:10.12454/j.jsuese.202300995

本刊网刊

矩形高层建筑扭转向脉动风荷载空间相关性

袁家辉[1,2],陈水福[2*],夏俞超[3],刘　奕[2]

(1.中冶南方城市建设工程技术有限公司,湖北 武汉 430063; 2.浙江大学 建筑工程学院,浙江 杭州 310058;
3.浙江东南网架股份有限公司,浙江 杭州 311209)

摘　要:为探讨建筑深宽比和来流湍流特性对矩形高层建筑扭转向脉动风荷载空间相关性的影响,在4种风场中对深宽比为1/9.0～9.0的矩形高层建筑进行同步测压风洞试验。基于试验结果,分析建筑深宽比、湍流强度和湍流积分尺度对扭转向脉动风荷载竖向相关系数和相干函数的影响;通过非线性最小二乘法,拟合得到适用于深宽比为1/9.0～9.0的矩形高层建筑竖向相关性数学模型。结果表明:扭转向脉动风荷载相关系数随着测点层高差增大呈指数衰减,衰减速率随着深宽比变化;扭转向脉动相干函数的初值与建筑深宽比和高差有关;对于深宽比大于1/5.0、小于等于5.0的建筑,相干函数存在明显谱峰,峰值对应折算频率与斯托罗哈数基本一致;来流湍流特性对相干函数的初值会有影响;针对不同风场提出的矩形高层建筑扭转向脉动风荷载相关系数和相干函数公式和试验结果吻合良好,可为建筑结构设计及荷载规范修订提供参考。

关键词:矩形高层建筑;扭转向脉动风荷载;空间相关性;风洞试验;深宽比;数学模型

中图分类号:TU312　　**文献标志码**:A　　**文章编号**:2096-3246(2025)06-0178-13

目前,中国新建的高层建筑绝大部分是住宅。板式高层住宅因居住容量大、造价低、施工方便、采光通风效果好和户型规整方正等优势在中国得到较多应用。典型板式高层住宅的截面形式近似为矩形,高度一般为百米左右,短边尺寸为十几米左右,长边尺寸从二十几米到近百米不等[1]。这种形式的高层建筑因为长边尺寸较大,受风荷载的影响更加显著,风振舒适度往往是结构设计的控制因素。脉动风荷载的空间相关性是风振计算中的重要参数。Davenport[2]、Shiotani[3]和Krenk[4]等采用顺风向脉动风速相干函数代替顺风向脉动风荷载相干函数。顾明[5]、曾加东[6]和袁家辉[7]等基于矩形高层建筑的同步测压风洞试验,提出了各自的顺风向脉动风荷载函数模型。Vickery等[8]研究高耸结构横风向脉动风荷载的空间相关性,提出了不包含频率项的横风向脉动风荷载相干函数经验公式。Liang[9]、顾明[10]和唐意[11]等基于矩形高层建筑的同步测压风洞试验,提出了横风向脉动风荷载函数模型。魏奇科等[12]对某295 m超高层建筑进行同步测压风洞试验,给出了考虑旋涡脱落影响的横风向脉动风荷载相干函数模型。

为更准确地计算扭转向的风振响应,国内外学者对扭转向脉动风荷载的空间相关性做了部分探索。Liang等[13]参考Vickery等[8]提出的横风向、扭转向脉动风荷载相干函数公式,对深宽比为1/4～4、高宽比为4～8的矩形截面高层建筑进行了同步测压风洞试验。顾明[14]和唐意[15]等对深宽比为1/3～3的矩形截面高层建筑进行同步测压风洞试验,分析不同深宽比建筑的扭转向脉动风荷载空间相关性,提出了相关系数的经验公式。黄东梅[16–17]、Huang[18]等对某492 m超高层建筑进行同步测压风洞试验,分析建筑不同高度的扭转向脉动风荷载相干函数,提出了对应的经验公式。上述典型扭转向相干函数经验公式,如表1所示。表1中,z_i、z_j分别为点i、j处的高度,B为建筑迎风面宽度,A_1、A_2为幅值修正系数,f为频率,f_1为折算频率,S_t为斯

收稿日期:2023－12－05　　**修回日期**:2024－05－07　　**网络出版日期**:2024－05－24

基金项目:国家自然科学基金项目(51878607)

作者简介:袁家辉(1996—),男,工程师,博士. 研究方向:建筑结构抗风. E-mail:yuanjiahui@zju.edu.cn

* **通信作者**:陈水福,教授,E-mail:csf@zju.edu.cn

托罗哈数，$\overline{U}_{Hr}$为建筑顶部平均风速，$\overline{U}$、$\bar{z}$分别为点i、j之间的平均风速和平均高度，H_r为建筑顶部高度，x为折算高度系数，α_1为折减系数，α_2、c_1、c_2为衰减系数。

由表1可以看出，以上相干函数模型都是根据特定建筑模型或小范围深宽比矩形高层建筑模型的风洞试验数据得到，无法排除特殊建筑截面形式对相干函数的影响，对目前最为常见的大深宽比矩形高层建筑可能不适用。另外，Liang[13]和唐意[15]等的相干函数模型形式简单，但本质是时域内的相关系数，不能反映相干函数随频率变化的特性。

为获得适用范围更广泛、实用性更佳的高层建筑扭转向脉动风荷载相关性的数学模型，给建筑结构荷载规范的修订提供参考。本文探讨正交风向下深宽比为1/9.0～9.0的矩形截面高层建筑扭转向脉动风荷载的相关系数及相干函数特性，总结相关系数和相干函数随建筑深宽比和风场类别的变化规律，然后通过最小二乘法和归纳分析方法获得相关系数及相干函数的数学模型。

表1　典型扭转向相干函数经验公式

Tab. 1　Empirical formula of typical torsional coherence function

文献	扭转向相干函数f_{coh}公式	参数取法
Liang等[13]	$f_{coh}(z_i,z_j)=\cos\left(\alpha_1\frac{\lvert z_i-z_j\rvert}{B}\right)\exp\left(-\left(\frac{\lvert z_i-z_j\rvert}{\alpha_2 B}\right)^2\right)$	α_1、α_2取值与建筑深宽比有关
唐意等[15]	$f_{coh}(z_i,z_j)=\cos\left(\alpha_1\frac{\lvert z_i-z_j\rvert}{B}\right)\exp\left(-\alpha_2\frac{\lvert z_i-z_j\rvert}{B}\right)$	α_1、α_2取值与建筑深宽比及风场类别有关
黄东梅等[18]	$f_{coh}(z_i,z_j,f)=A_1\exp(-c_1f_1)+A_2\exp\left(-(f_1-S_t\frac{\lvert z_i-z_j\rvert}{B}\cdot\frac{\overline{U}_{Hr}}{\overline{U}})^2\Big/c_2^2\right)$	$f_1=f\lvert z_i-z_j\rvert/\overline{U}, S_t=0.162, x=\frac{\lvert z_i-z_j\rvert/H_r}{(\bar{z}/H_r)^5}$, $A_1=\exp\left(-3.96\lvert z_i-z_j\rvert/H_r\right), A_2=0.552\left(x^2+14.5x\right)/\left(x^2+13.7x+1.07\right)$, $c_1=5.53\exp\left(-8.94\lvert z_i-z_j\rvert/H_r\right), c_2=\left(\frac{\bar{z}}{H_r}\right)^2\exp\left(-2.19-\frac{0.0789}{\lvert z_i-z_j\rvert/H_r+0.0099}\right)$

1　风洞试验

1.1　风场模拟

试验在加拿大西安大略大学边界层风洞Ⅱ的高速试验段中进行，该高速测试段宽为3.4 m、高为2.1 m、长为30.0 m。风洞入口处有系列全自动的湍流产生装置，包括粗糙元、齿形格栅、尖劈和挡板等。按照工程科学数据库（Engineering Sciences Data Unit）模拟O1、S1、O2和S2这4种风场。其中，S类风场的湍流强度大于O类，1类风场的湍流积分尺度大于2类。具体的风场设置方法参见文献[19]。风速数据使用眼镜蛇3维脉动风速测量仪（TFI900311）采集，其采样频率为1 250 Hz，本次试验风速采样时间为30 s。平均风速剖面按照标准ESDU—85020[20]推荐的对数率公式模拟，理论值计算式为：

$$\frac{\overline{U}_z}{\overline{U}_{10}}=\frac{\ln(z/z_0)}{\ln(10/z_0)}+\frac{86.25f_c z}{\overline{U}_{10}} \tag{1}$$

式中，z为高度，$\overline{U}_z$为z处的平均风速，$\overline{U}_{10}$高度为10 m处的平均风速，z_0为地表粗糙长度，f_c为科里奥利力，试验O1、S1、O2和S2风场在模型顶部的缩尺平均风速分别为8.86、8.32、8.07和8.11 m/s。

湍流强度的剖面理论值I_{uz}按照标准ESDU—82026[21]推荐的计算式进行模拟：

$$I_{uz}=\frac{7.5\eta u^*\left(0.538+0.09\ln(z/z_0)\right)^p}{\left(1+0.156\ln(u^*/f_c z_0)\right)\overline{U}_z} \tag{2}$$

式中，η、p为拟合参数，u^*为摩擦速度，O1、S1、O2和S2风场在模型顶部的湍流强度分别为0.124、0.187、0.122和0.170。

湍流积分尺度按标准ESDU—74031[22]建议的公式进行模拟：

$$L_u=\overline{U}_z\int_0^{\tau_0}\rho_{uu}(\tau)\mathrm{d}\tau \tag{3}$$

式中，L_u为湍流积分尺度，ρ_{uu}为脉动风速自相关系数，τ为时差，τ_0为自相关系数收敛至0时对应的时差，O1、S1、O2和S2风场在模型顶部的缩尺湍流积分尺度分别为1.328、1.545、0.504和0.656 m。

4种不同风场的平均风速和湍流度剖面如图1所示。图1中，z_0为各风场足尺地表粗糙长度，α为指数率形式的剖面参数，$\overline{U}_H$为建筑顶部平均风速。由图1可知，试验值和理论值拟合情况良好。

脉动风速谱模拟采用标准ESDU—74031[22]建议的von–Karman谱模拟：

$$\begin{cases} \dfrac{fS_{uu}(f)}{\sigma_u^2} = \dfrac{4f_u}{\left(1+70.8f_u^2\right)^{5/6}}, \\ f_u = \dfrac{fL_u}{\overline{U}_z} \end{cases} \tag{4}$$

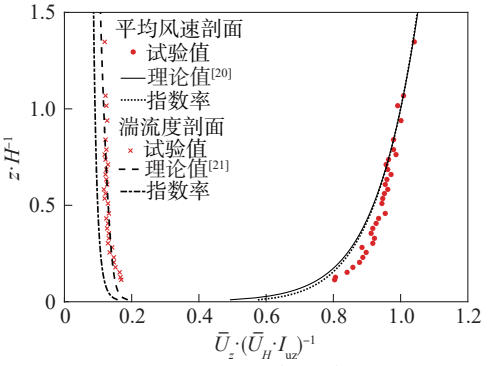

(a) O1, z_0 = 0.01 m（足尺）, α= 0.12

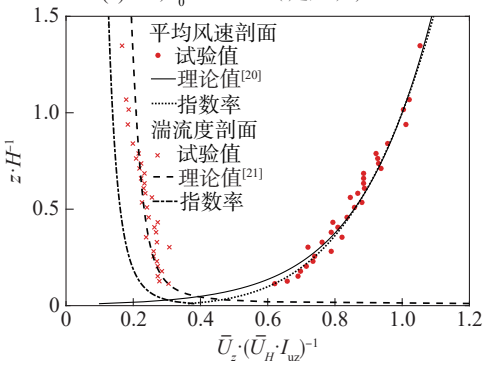

(b) S1, z_0 = 0.60 m（足尺）, α= 0.22

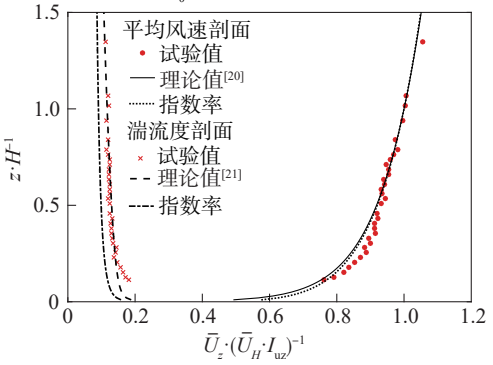

(c) O2, z_0 = 0.01 m（足尺）, α= 0.12

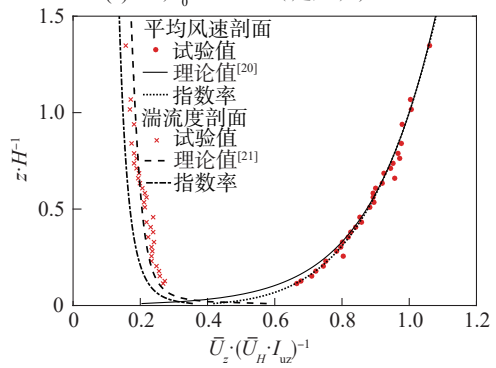

(d) S2, z_0 = 0.30 m（足尺）, α= 0.19

图1 4种不同风场的平均风速和湍流度剖面

Fig. 1 Mean velocity and turbulence intensity profiles for 4 different wind fields

式中，f_u为折算频率，S_{uu}为脉动风速的功率谱密度，σ_u为脉动风速的标准差。

图2为本次风洞试验4种风场在z=0.762H高度处脉动风速谱的试验值和理论值，可见二者吻合良好。

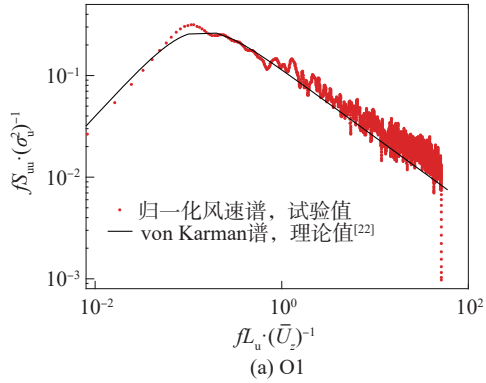

(a) O1

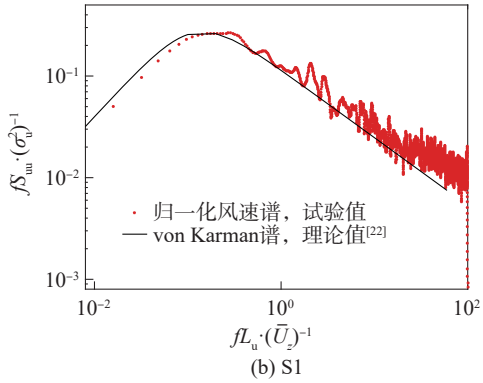

(b) S1

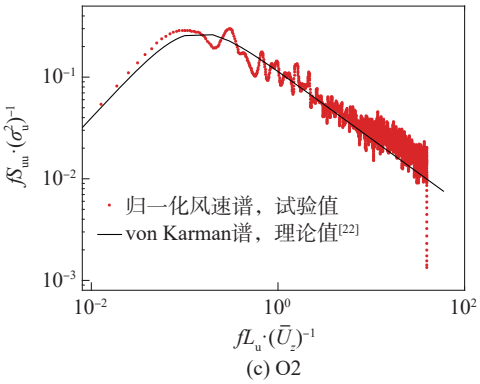

(c) O2

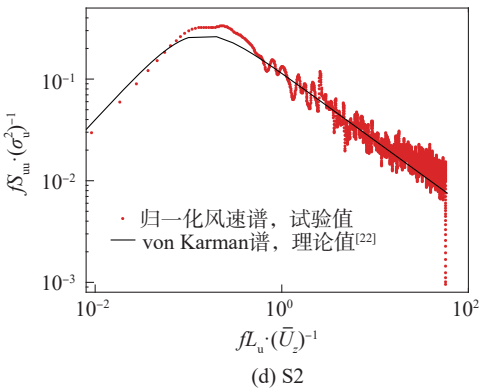

(d) S2

图2 4种风场在z=0.762H高度处脉动风速谱的试验值和理论值

Fig. 2 Experimental and theoretical values of fluctuating velocity Spectra at z=0.762H for 4 wind

1.2　试验模型

测压试验采用缩尺比为 1∶200 的刚性节段模型，模型高为 0.50 m，宽为 0.06 m，长为 0.06～0.54 m。模型共有 12 段，其中，段 1～6 的长宽比为 0.5，段 7～12 的长宽比为 1.0。沿高度方向布置 7 个测点层，分别位于 0.10H、0.30H、0.50H、0.65H、0.80H、0.90H 和 0.98H 高度处，测点层从低到高编号分别为 1#～7#，各测点层的布置方式相同，模型平面图与测点布置如图 3 所示。定义模型的深宽比为 D/B，其中，D 为侧风面深度。短边迎风时深宽比大于等于 1.0，长边迎风时深宽比小于等于 1.0。深宽比为 1/9.0 的模型进行试验时阻塞效应最大，根据模型尺寸和风洞测试段尺寸计算出阻塞比约为 3.8%（小于 5.0%），本次试验可忽略阻塞效应[23]。通过不同的拼接方式可以得到深宽比为 1/9.0～9.0 的试验模型，具体拼接方式和试验模型参数如表 2 所示。针对每种深宽比模型进行测压试验，采样频率为 400 Hz，采样时间为 90 s。风洞试验过程照片如图 4 所示。

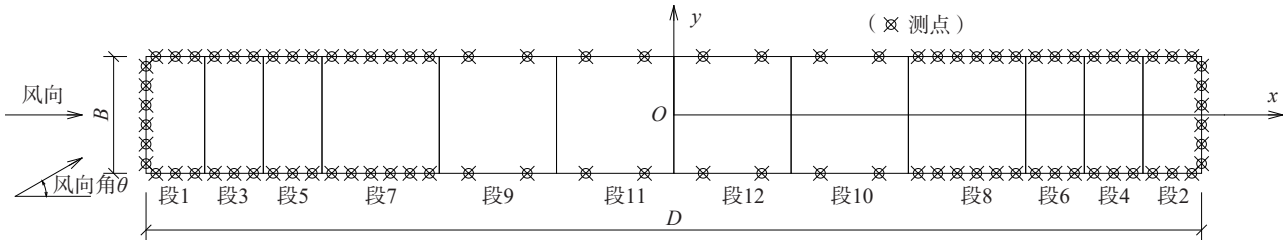

图3　模型平面图与测点布置

Fig. 3　Plan sketch of model and layout of pressure taps

表2　试验模型参数

Tab. 2　Parameters of experiment models

风场类型	深宽比	拼接方式（从左至右）	测压点数
O1	1/9.0,9.0	1,3,5,7,9,11,12,10,8,6,4,2	616
O1,O2,S1,S2	1/8.0,8.0	1,3,5,7,9,11,10,8,6,4,2	588
O1	1/7.0,7.0	1,3,5,7,9,10,8,6,4,2	560
O1	1/6.0,6.0	1,3,5,7,10,8,6,4,2	532
O1,O2,S1,S2	1/5.0,5.0	1,3,5,7,8,6,4,2	504
O1	1/4.0,4.0	1,3,5,7,6,4,2	420
O1,O2,S1,S2	1/3.0,3.0	1,3,5,6,4,2	336
O1	1/2.5,2.5	1,3,5,4,2	294
O1,O2,S1,S2	1/2.0,2.0	1,3,5,2	252
O1	1/1.5,1.5	1,4,2	210
O1,O2,S1,S2	1.0	1,2	168

图4　风洞试验过程照片

Fig. 4　Wind tunnel test photos

2　脉动风荷载空间相关性分析

2.1　相关系数特性

扭转向脉动风荷载相关系数 $f_{\mathrm{cor}}(z_i,z_j)$ 为：

$$f_{\mathrm{cor}}(z_i,z_j)=\frac{\mathrm{cov}\left(F_{\mathrm{T}}(z_i),F_{\mathrm{T}}(z_j)\right)}{\sigma(z_i)\sigma(z_j)} \tag{5}$$

式中，$F_{\mathrm{T}}(z_i)$ 和 $F_{\mathrm{T}}(z_j)$ 分别为 z_i 和 z_j 高度处的测点层扭转向气动力，$\sigma(z_i)$ 和 $\sigma(z_j)$ 分别为 $F_{\mathrm{T}}(z_i)$ 和 $F_{\mathrm{T}}(z_j)$ 的标准差，cov 为协方差函数。

O1 风场下扭转向脉动风荷载相关系数如图 5 所示。由图 5 可知，扭转向脉动风荷载相关系数受建筑深宽比和测点层高差 $\Delta z(\Delta z=|z_i-z_j|)$ 影响。随着测点层高差增大，相关系数基本呈指数衰减。当 $D/B\leq1.0$ 时，所有建筑的相关系数都大于 0，相关系数衰减速率随深宽比增大而增大，这可能是因为：当 $D/B\leq1.0$ 时，随着建筑深宽比增大，背风面宽度减小，侧风面受到背风面回流的干扰增大，因此相关性减弱；当 $D/B>1.0$ 时，相关系数衰减速率随深宽比增大而减小；部分建筑在测点层高差较大位置的相关系数会出现负值，这是因为随着建筑深宽比增大，侧风面长度增大，从建筑前缘分离的气流会在侧风面再附并形成滚动的涡[24–25]，再附后的气流相较于分离的气流更加稳定，相关性增强，此时扭转向脉动风荷载相关系数的离散性明显大于 $D/B\leq1.0$ 的工况。离散性大致呈现 3 个阶段变化：1）$1.0<D/B<3.0$，相关系数离散性基本不变；2）$3.0\leq D/B<5.0$，离散性逐渐增大；3）$5.0\leq D/B\leq9.0$，离散性逐渐减小。这是因为矩形高层建筑的再附长度约等于 3 倍的迎风面宽度[26]，再附过程增强了相关系数的离散性，再附结束后相关系数趋于稳定。

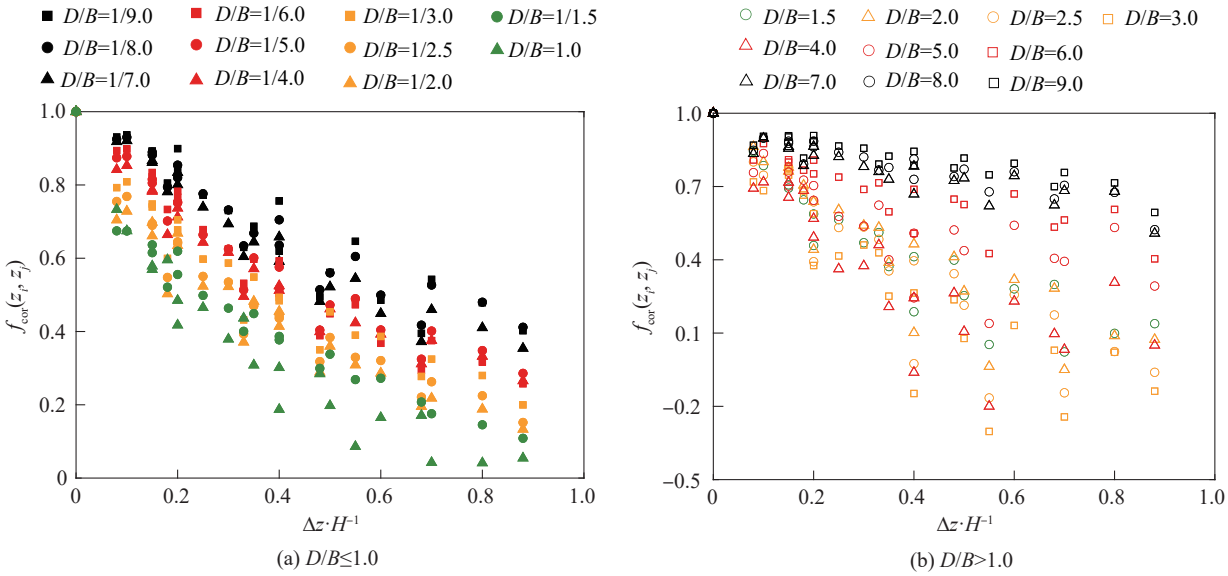

(a) $D/B \leq 1.0$ (b) $D/B > 1.0$

图 5 O1 风场下扭转向脉动风荷载相关系数

Fig. 5 Correlation coefficients of torsional fluctuating wind loads in O1 wind field

为考察来流湍流特性对扭转向脉动风荷载相关系数的影响，定义湍流积分尺度影响系数为 O1 与 O2 风场下扭转向脉动风荷载相关系数的比值，定义湍流强度影响系数为 S1 与 O1 风场下扭转向脉动风荷载相关系数比值，计算公式为：

$$\begin{cases} R_{\mathrm{T}}^{L_{\mathrm{u}}} = \dfrac{f_{\mathrm{cor}}^{\mathrm{O1}}}{f_{\mathrm{cor}}^{\mathrm{O2}}}, \\ R_{\mathrm{D}}^{I_{\mathrm{u}}} = \dfrac{f_{\mathrm{cor}}^{\mathrm{S1}}}{f_{\mathrm{cor}}^{\mathrm{O1}}} \end{cases} \tag{6}$$

式中，$R_{\mathrm{T}}^{L_{\mathrm{u}}}$ 为湍流积分尺度影响系数，$R_{\mathrm{D}}^{I_{\mathrm{u}}}$ 为湍流强度影响系数，$f_{\mathrm{cor}}^{\mathrm{O1}}$ 为 O1 风场下扭转向脉动风荷载相关系数，$f_{\mathrm{cor}}^{\mathrm{O2}}$ 为 O2 风场下扭转向脉动风荷载相关系数，$f_{\mathrm{cor}}^{\mathrm{S1}}$ 为 S1 风场下扭转向脉动风荷载相关系数。

湍流特性对扭转向脉动风荷载相关系数影响如图 6 所示。由图 6 可观察到，扭转向脉动风荷载相关系数的湍流特性影响系数变化规律同时受建筑深宽比和测点层高差的影响。当 $D/B<1.0$ 时，测点层高差的变化对湍流积分尺度和湍流强度影响系数的影响较小，这是因为此时扭转向脉动风荷载主要由背风面的风压不均匀分布控制，来流的湍流特性不是主要影响因素；当 $D/B \geq 1.0$ 时，测点层高差较小时，湍流积分尺度和湍流强度影响系数约等于 1.0，表明湍流积分尺度和湍流强度对脉动风荷载相关系数都无明显影响。测点层高差较大时，湍流积分尺度和强度影响系数在 1 附近波动，可能会出现负值，此时扭转向脉动风荷载由侧风面的风力不对称作用和背风面的风压不均匀分布共同产生，来流的湍流特性会影响来流的分离、再附和旋涡脱落[27]。

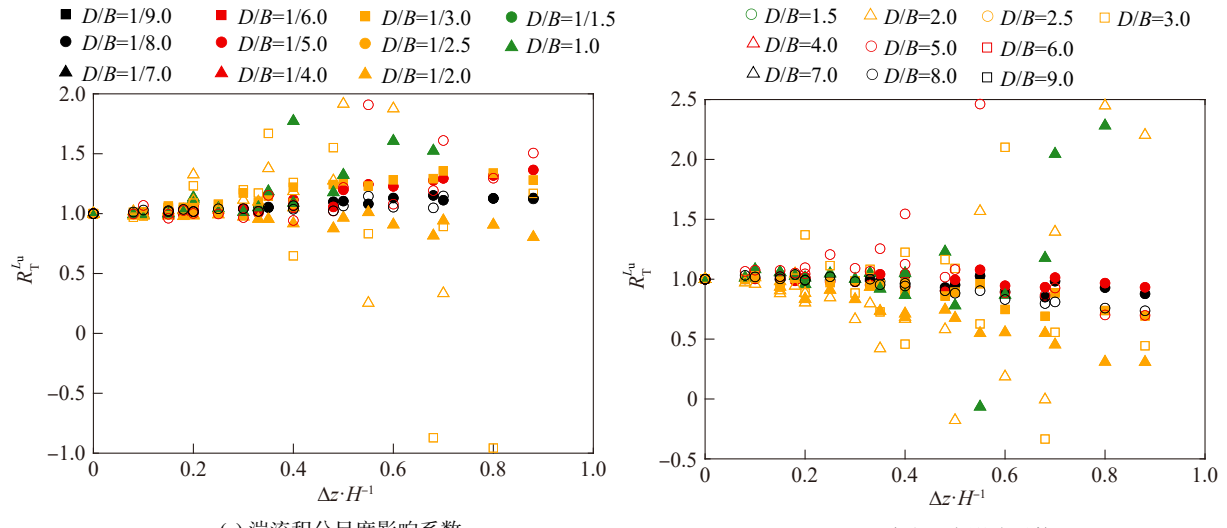

(a) 湍流积分尺度影响系数 (b) 湍流强度影响系数

图 6 湍流特性对扭转向脉动风荷载相关系数的影响

Fig. 6 Effects of turbulence characteristics on correlation coefficients of torsional fluctuating wind loads

2.2　相干函数特性

扭转向脉动风荷载相干函数$f_{\mathrm{coh}}(z_i,z_j,f)$为：

$$f_{\mathrm{coh}}(z_i,z_j,f)=\frac{\mathrm{Re}\left(S_{\mathrm{T}}(z_i,z_j,f)\right)}{\sqrt{S_{\mathrm{T}}(z_i,f)S_{\mathrm{T}}(z_j,f)}} \tag{7}$$

式中，$\mathrm{Re}(S_{\mathrm{T}}(z_i,z_j,f))$为高度$z_i$和$z_j$处测点层扭转向脉动风荷载互功率谱实部，$S_{\mathrm{T}}(z_i,f)$和$S_{\mathrm{T}}(z_j,f)$分别为高度$z_i$和$z_j$处测点层扭转向脉动风荷载自功率谱。

O1 风场扭转向脉动风荷载相干函数如图 7 所示。图 7 中，3# vs 4#表示测点层 3#和 4#的对比，下同。观察图 7 可知，扭转向脉动风荷载相干函数存在以下特性：1）频率为 0 时，相干函数值与建筑深宽比和高差有关。2）对于 1/5.0≤D/B≤5.0 的建筑，相干函数的谱峰比较明显；当 D/B≤1.0 时，峰值对应折算频率$fB/\overline{U}_H$略大于 0.1，与斯托罗哈数基本一致，此时谱峰是由旋涡脱落造成的；当 D/B>1.0 时，峰值对应折算频率逐渐减小。3）不同深宽比建筑相干函数随频率变化规律不同：当 D/B≤1.0 时，相干函数先减小后增大，达到峰值后迅速减小到低相干水平；当 1.0<D/B≤5.0 时，高差较大的相干函数随频率缓慢减小，高差较小的相干函数在低相干水平反复波动；当 D/B>5.0 时，相干函数随频率快速衰减，然后在低相干水平波动。4）扭转向脉动风荷载相干函数变化规律复杂，Δz 和 $\overline{U}$ 都会对相干函数变化趋势产生影响。

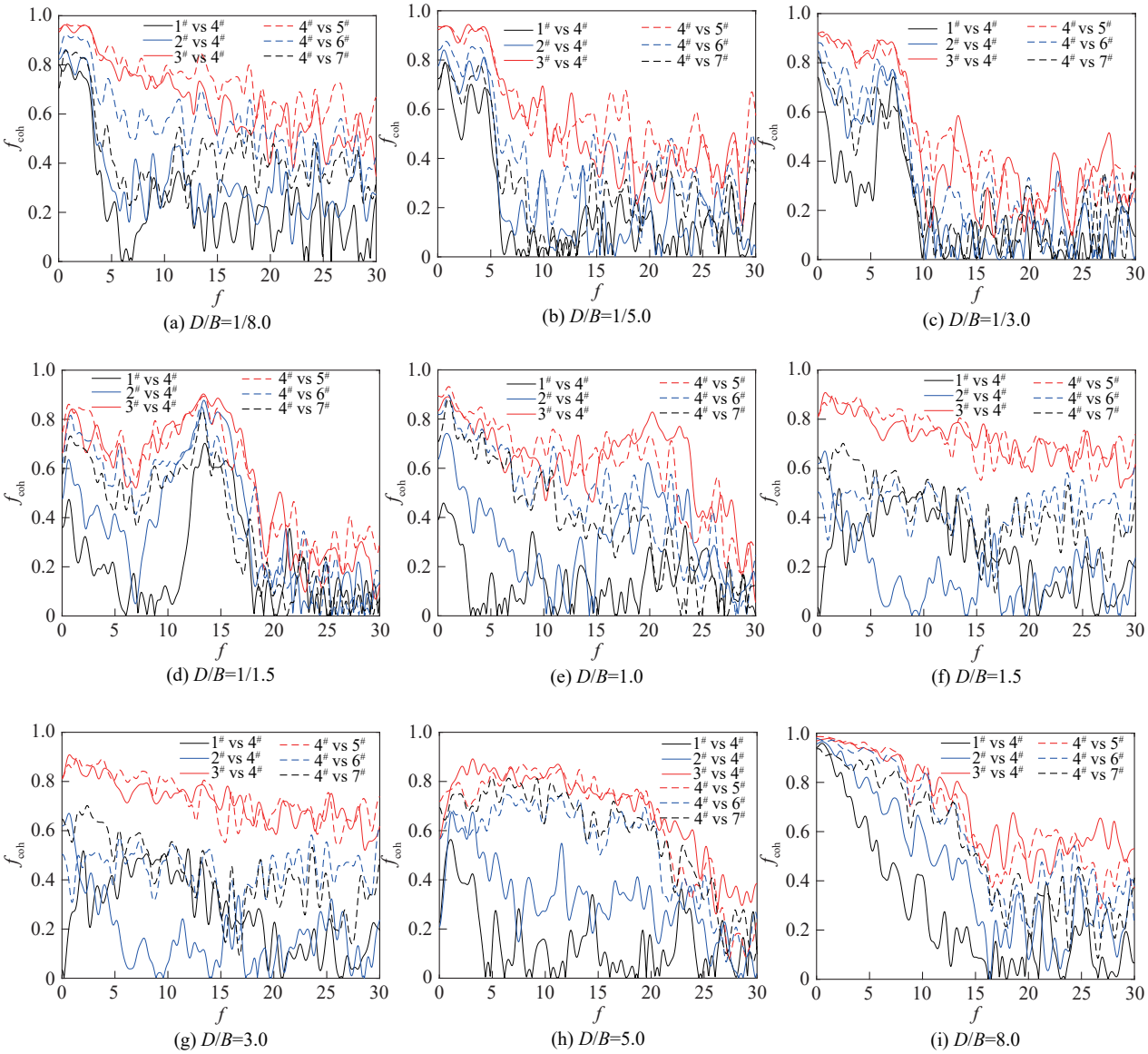

图 7　O1 风场下扭转向脉动风荷载相干函数

Fig. 7　Coherence functions of torsional fluctuating wind loads in O1 wind field

不同风场下扭转向脉动风荷载相干函数如图 8 所示。图 8 以测点层 3# vs 4#的相干函数为例进行分析。由图 8 可观察到，来流湍流特性对扭转向脉动风荷载相干函数的初值影响较大；在不同风场中，相干函数随频率和建筑深宽比的波动很大，湍流积分尺度和湍流强度对扭转向脉动风荷载相干函数的影响并不呈现明显规律。

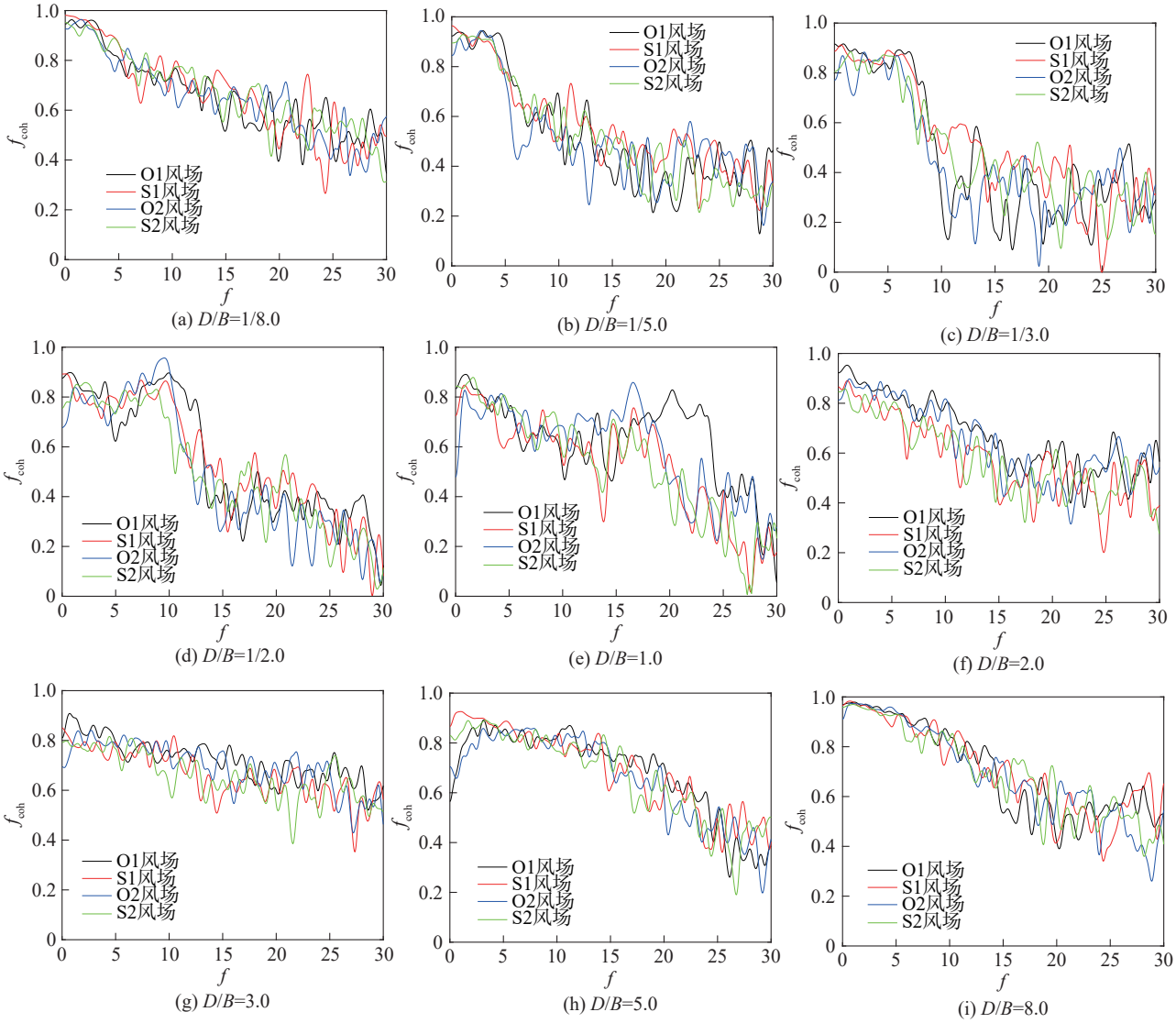

图8 不同风场下扭转向脉动风荷载相干函数

Fig. 8 Coherence functions of torsional fluctuating wind loads in different wind fields

3 脉动风荷载相关性数学模型

3.1 相关系数数学模型

扭转向脉动风荷载相关系数和测点层高差、建筑深宽比及风场类别均有关系。在D/B≤1.0时，所有建筑的扭转向脉动风荷载相关系数都大于0；在D/B>1.0时，部分建筑在测点层高差较大位置的相关系数会出现负值。根据第2.1节曲线呈现的变化形式，同时参考文献[13,15]，本文选取指数形式公式基础上考虑幅值修正系数的公式作为扭转向脉动风荷载相关系数的拟合式，并采用最小二乘法进行拟合，其拟合式为：

$$f_{\mathrm{cor}}(z_i,z_j)=\cos\left(p_1\frac{\Delta z}{B}\right)\exp\left(-p_2\frac{\Delta z}{B}\right) \tag{8}$$

式中，p_1、p_2为待拟合参数。

对于不同风场类别下、不同深宽比建筑，拟合式的参数为：

$$p_1=\begin{cases}0.143s^2+(-0.367t^2+1.87t-2.34)s+0.8t^2-\\ \quad 3.73t+3.91, 2\le s\le 4;\\ 0, s<2,\ s>4\end{cases} \tag{9}$$

$$p_2=\begin{cases}10^{-2}(2.3t^3-16.7t^2+37.1t+19.5)s^{(0.069t^3-0.533t^2+1.21t-1.2)},\\ \quad s\le 3;\\ 10^{-3}(3.6t^3-29.5t^2+75.5t-37.6)s^2-\\ \quad 10^{-2}(3.5t^3-29t^2+77t-31)s-0.095t^2+\\ \quad 0.59t+0.43, s>3\end{cases} \tag{10}$$

式中：t为风场类别；O1、S1、O2和S2风场分别取1、2、3和4；s为建筑深宽比，取值范围为1/9.0～9.0。

O1风场下扭转向脉动风荷载相关系数公式拟合参数与计算值比较如图9所示，其拟合曲线与试验值比较，如图10所示。由图9可知，式(8)的拟合参数与式(9)～(10)的计算值比较，计算值与离散的拟合参

数误差很小。图 10 检验了式(8)～(10)的准确性，拟合曲线和试验值吻合良好，说明式(8)～(10)组成的闭合求解公式可以反映扭转向脉动风荷载相关系数随高差的变化关系。

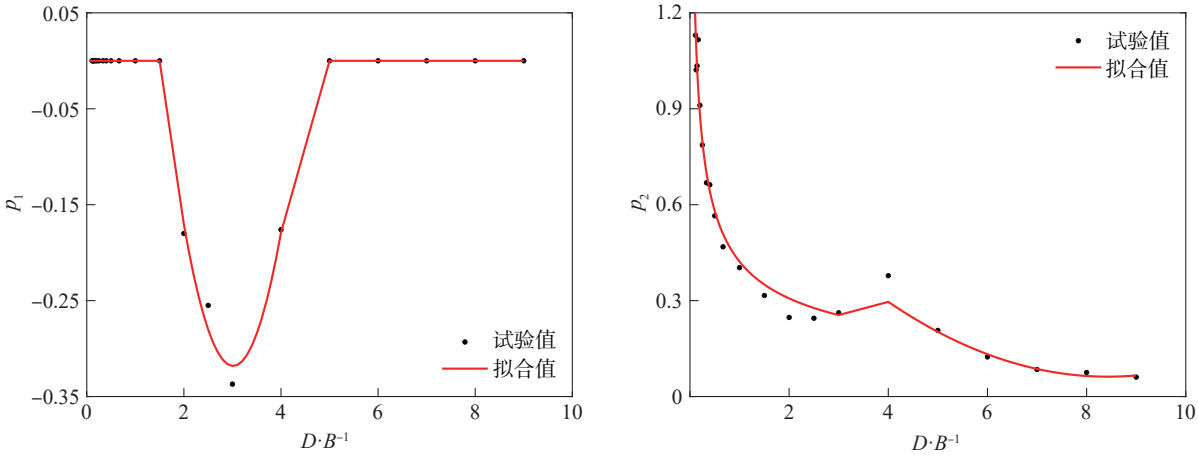

(a) 参数p_1拟合　　(b) 参数p_2拟合

图 9　O1 风场下扭转向脉动风荷载相关系数公式拟合参数与计算值比较

Fig. 9　Comparison of fitting and calculated values of correlation coefficient formula parameters in O1 wind field

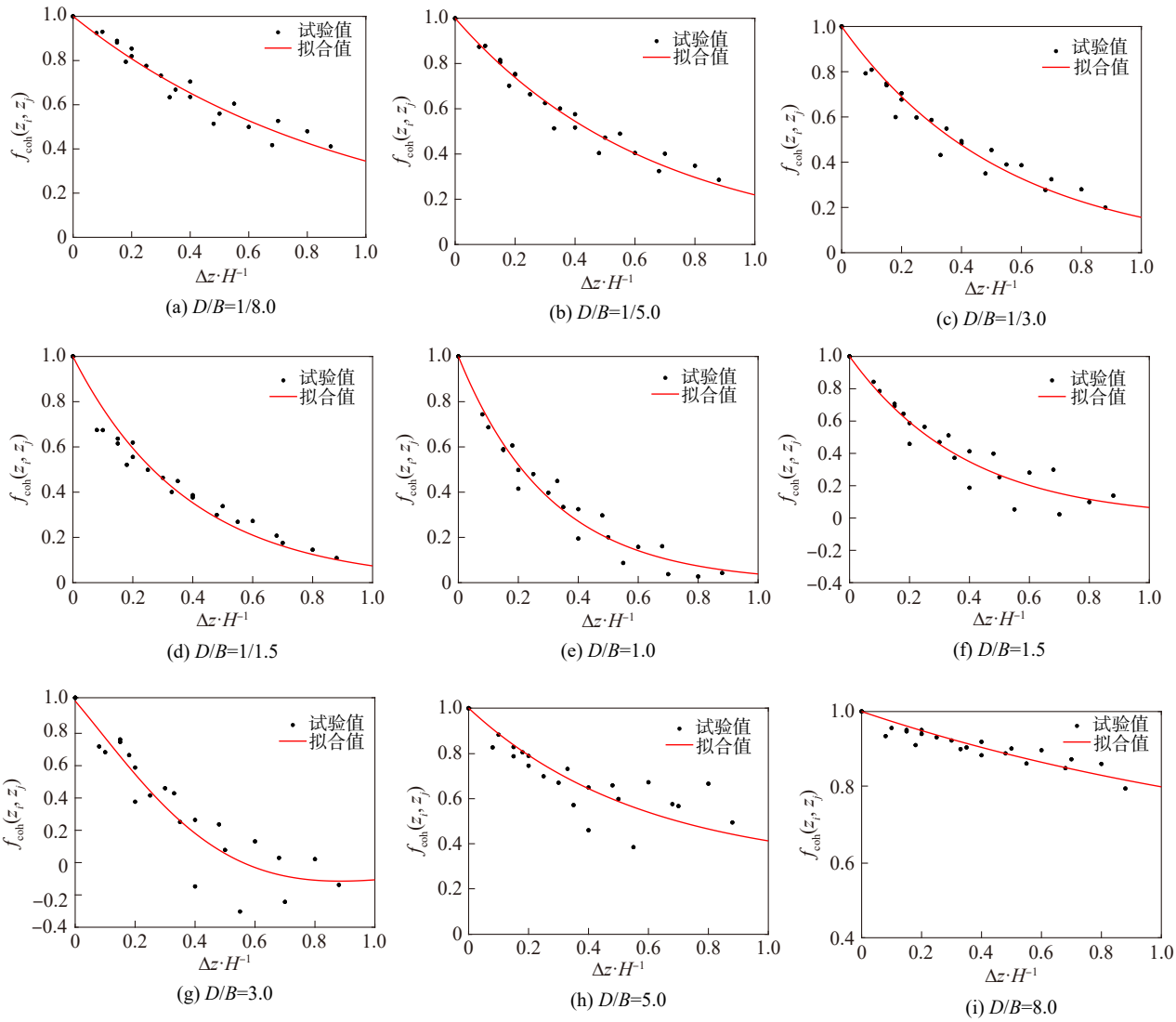

(a) D/B=1/8.0　(b) D/B=1/5.0　(c) D/B=1/3.0

(d) D/B=1/1.5　(e) D/B=1.0　(f) D/B=1.5

(g) D/B=3.0　(h) D/B=5.0　(i) D/B=8.0

图 10　O1 风场下扭转向脉动风荷载相关系数拟合值与试验值比较

Fig. 10　Comparison of fitting and experimental values of torsional fluctuating wind loads in O1 wind field

3.2 相干函数数学模型

扭转向脉动风荷载相干函数和频率、测点层高差、平均风速、建筑深宽比及风场类别均有关系。对于1/5.0≤D/B≤5.0的建筑，相干函数存在较为明显的谱峰。为了便于工程应用，参考文献[18]中相干函数的形式，选取式(11)的曲线形式作为横风向脉动风荷载相干函数的基础拟合式，再探究幅值修正系数和衰减系数与建筑深宽比及风场类别等因素的拟合关系式为：

$$f_{\mathrm{coh}}(z_i,z_j,f)=A_1\exp(-c_1\frac{f\Delta z}{\overline{U}})+A_2\exp(-c_2\frac{|f-f_{\mathrm{s}}\overline{U}_H/B|\Delta z}{\overline{U}}) \tag{11}$$

式中，$\overline{U}=(\overline{U}_i+\overline{U}_j)/2$，$f_{\mathrm{s}}$为峰值对应折算频率。

建筑扭转向脉动风荷载相干函数谱峰对应折算频率f_{s}取值如表3所示。

表3 建筑扭转向脉动风荷载相干函数谱峰对应折算频率f_{s}取值

Tab. 3 Reduced frequencies to peaks of torsional fluctuating wind load coherence functions

D/B	1/9.0	1/8.0	1/7.0	1/6.0	1/5.0	1/4.0	1/3.0	1/2.5	1/2.0	1/1.5	1.0	1.5	2.0	2.5	3.0	4.0	5.0	6.0	7.0	8.0	9.0
f_{s}	0	0	0	0	0.152	0.144	0.142	0.141	0.141	0.137	0.134	0.092	0.071	0.060	0.043	0.033	0.030	0	0	0	0

本次风洞试验模型竖向共7个测点层，每种工况下的模型存在21个扭转向脉动风荷载相干函数。考虑O1、S1、O2和S2这4种风场及建筑深宽比的变化，共拟合1 008个相干函数。O1风场下部分扭转向脉动风荷载相干函数拟合结果如图11所示。

图11给出了曲线对应的实验工况平面简图、测点层高差和平均风速，其中，箭头代表风向，矩形代表模型，数字为模型的实际尺寸。由图11可知，式(11)能大致拟合不同深宽比建筑不同测点层之间的扭转向脉动风荷载相干函数。

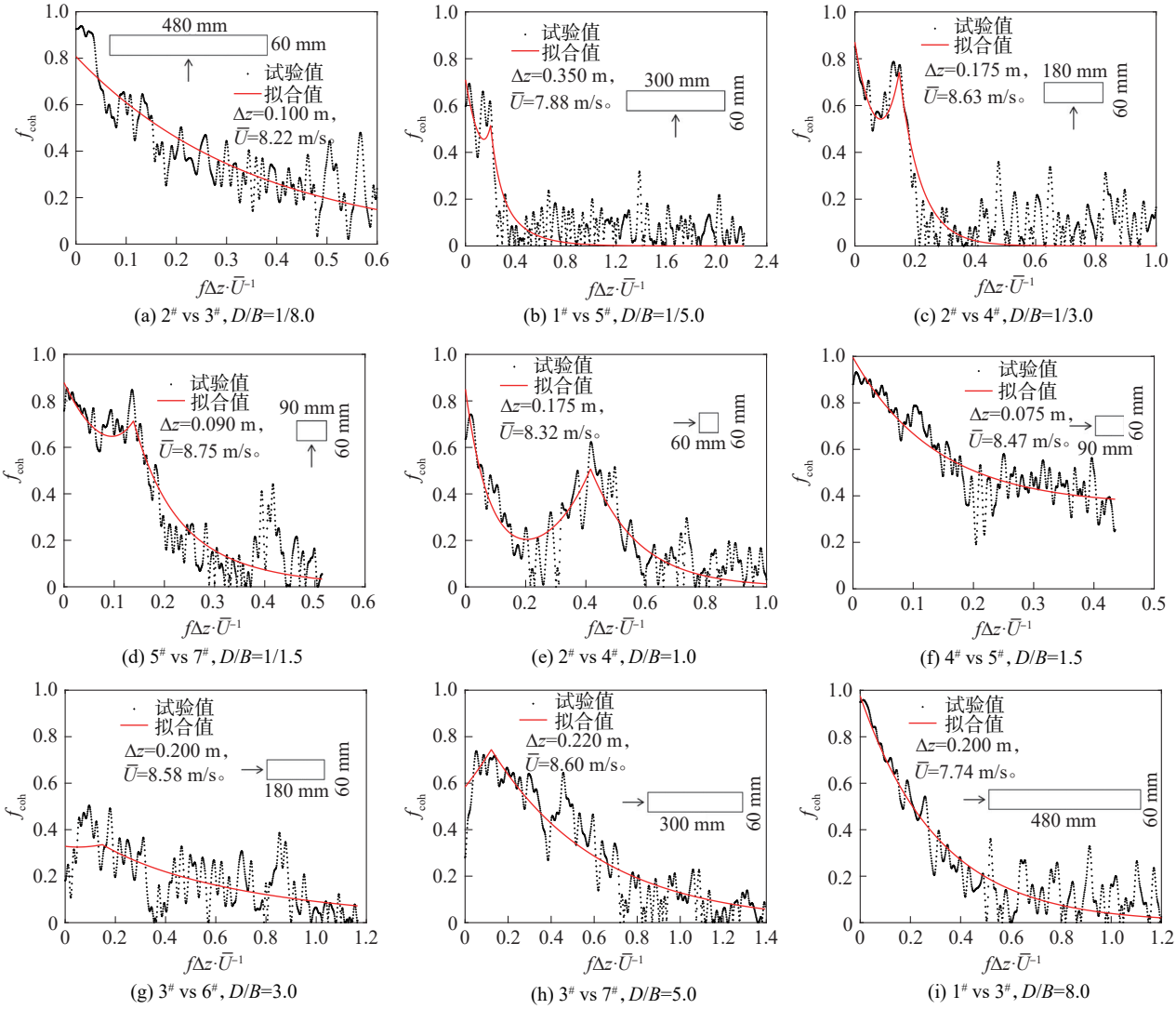

(a) 2# vs 3#，D/B=1/8.0 (b) 1# vs 5#，D/B=1/5.0 (c) 2# vs 4#，D/B=1/3.0

(d) 5# vs 7#，D/B=1/1.5 (e) 2# vs 4#，D/B=1.0 (f) 4# vs 5#，D/B=1.5

(g) 3# vs 6#，D/B=3.0 (h) 3# vs 7#，D/B=5.0 (i) 1# vs 3#，D/B=8.0

图11 O1风场下部分扭转向脉动风荷载相干函数拟合结果

Fig. 11 Some coherence function fitting results of torsional fluctuating wind loads in O1 wind field

根据反复试算和分析，并结合文献[5]中对衰减系数的分析方式，以测点层高差与平均高度的比值 $\Delta z/\bar{z}$ 为变量的线性公式描述不同测点层之间的幅值修正系数 A_1、A_2 和衰减系数 c_1、c_2，如式（12）所示：

$$\begin{cases} A_1 = p_1\dfrac{\Delta z}{\bar{z}} + p_2, \\ c_1 = p_3\dfrac{\Delta z}{\bar{z}} + p_4, \\ A_2 = p_5\dfrac{\Delta z}{\bar{z}} + p_6, \\ c_2 = p_7\dfrac{\Delta z}{\bar{z}} + p_8 \end{cases} \tag{12}$$

式中，p_3～p_8为待拟合参数，$\bar{z}$为测点层平均高度。

第二次拟合得到不同深宽比建筑的参数p_1～p_8，以建筑深宽比为变量拟合参数p_1～p_8的表达式。不同风场下扭转向脉动风荷载相干函数的参数差距较大，需要分别拟合。不同风场、不同深宽比建筑扭转向脉动风荷载相干函数参数计算如式（13）～（20）所示：

$$p_1 = \begin{cases} (-0.005t + 0.071)s^2 + (0.02t^2 - 0.077t - 0.088)s - \\ \quad 0.06t - 0.156, s \le 6; \\ -0.083t^3 + 0.64t^2 - 1.51t + 0.923, s > 6 \end{cases} \tag{13}$$

$$p_2 = \begin{cases} (0.012t^3 - 0.093t^2 + 0.213t - 0.32)s + 0.041t^3 - \\ \quad 0.31t^2 + 0.687t + 0.5, s \le 6; \\ 0.023\,3t^3 - 0.182t^2 + 0.437t + 0.729, s > 6 \end{cases} \tag{14}$$

$$p_3 = \begin{cases} (2.59t^3 - 20.2t^2 + 46.4t - 31.1)\ln s + 5.36t^3 - \\ \quad 41.8t^2 + 95.5t - 64, s \le 0.67; \\ (0.219t^3 - 1.7t^2 + 4.09t - 3.3)s - 0.959t^3 + \\ \quad 7.58t^2 - 18.77t + 16.6, s > 0.67 \end{cases} \tag{15}$$

$$p_4 = \begin{cases} (0.183t^2 - 1.25t + 2.87)\ln s + 0.576t^2 - \\ \quad 3.22t + 9.43, s \le 3; \\ (-2.32t^3 + 18.06t^2 - 42.4t + 31.2)\ln s + \\ \quad 4.23t^3 - 33.1t^2 + 77.8t - 53.8, s > 3 \end{cases} \tag{16}$$

$$p_5 = (0.026t^3 - 0.192t^2 + 0.423t - 0.42)s - 0.071t^3 + 0.51t^2 - 1.1t + 0.83 \tag{17}$$

$$p_6 = (0.010\,5t + 0.137)s - 0.067t^3 + 0.524t^2 - 1.25t + 0.97 \tag{18}$$

$$p_7 = \begin{cases} (3.2t^3 - 20.7t^2 + 50.1t - 44.3)s - 2.81t^3 + \\ \quad 20.9t^2 - 47.3t + 36.1, s \le 1; \\ (0.157t^3 - 1.1t^2 + 2.34t - 2.53)s - 0.628t^3 + \\ \quad 4.42t^2 - 9.59t + 8.03, s > 1 \end{cases} \tag{19}$$

$$p_8 = \begin{cases} (-4.57t^3 + 32.8t^2 - 71.7t + 47.6)s + \\ \quad 1.62t^3 - 11.86t^2 + 25.8t - 4.68, s \le 1; \\ (-0.12t^3 + 0.878t^2 - 2.05t + 2.75)s + \\ \quad 0.366t^3 - 2.61t^2 + 6.14t - 6.15, s > 1 \end{cases} \tag{20}$$

4　结　论

本文基于同步测压风洞试验，研究了4种风场下深宽比为1/9.0～9.0的矩形高层建筑扭转向脉动风荷载的竖相关系数和相干函数特性，拟合了适用于不同风场、不同深宽比建筑的相关系数和相干函数公式，得出以下结论：

1）当 $D/B \le 1.0$ 时，扭转向脉动风荷载相关系数大于0，相关系数衰减速率随长宽比增大而增大；当 $D/B > 1.0$ 时，扭转向脉动风荷载相关系数离散性非常大，相关系数衰减速率随深宽比增大而减小，部分建筑在测点层高差较大位置的相关系数会出现负值。

2）当 $D/B < 1.0$ 时，来流湍流特性对扭转向脉动风荷载相关系数影响很小；当 $D/B \ge 1.0$ 时，测点层高差较大时，来流湍流特性的变化会使相关系数出现负值。

3）当 $1/5.0 \le D/B \le 5.0$ 时，扭转向脉动风荷载相干函数上存在由旋涡脱落造成的谱峰，峰值对应折算频率与斯托罗哈数基本一致。

4）来流湍流特性对扭转向脉动风荷载相干函数的初值影响较大，在不同风场中，相干函数随频率和建筑深宽比的波动很大。

5）通过最小二乘法拟合得到的相关系数和相干函数系列闭合求解公式和试验值吻合良好，可为建筑结构设计及荷载规范修订提供参考。

参考文献：

[1] Liu Yi. Wind loads on slab-type high-rise buildings[D]. Hangzhou: Zhejiang University, 2019. [刘奕 . 板式高层建筑风荷载研究[D]. 杭州：浙江大学，2019.]

[2] Davenport A G. Gust loading factors[J]. Journal of the Structural Division, 1967, 93(3): 11–34.

[3] Shiotani M, Avai H. Lateral structures of gusts in high winds[C]//International Conference on the Wind Effect on Buildings and Structures, Cambridge: Cambridge University Press, 1967: 535–555.

[4] Krenk S. Wind field coherence and dynamic windforces[C]// IUTAM Symposium on Advances in Nonlinear Stochastic Mechanics, Dordrecht: Springer, 1996: 269–278.

[5] Gu Ming, Zhang Jianguo. Coherence analysis of along-wind fluctuating loads on high-rise buildings[J]. China Civil Engineering Journal, 2008, 41(11): 18–22. [顾明，张建国 . 高

层建筑顺风向脉动荷载相干性研究[J]. 土木工程学报, 2008,41(11):18–22.]

[6] Zeng Jiadong, Li Mingshui, Li Shaopeng. Spatial correlation analysis of fluctuating along-wind loads on high-rise buildings with rectangular section[J].Journal of Harbin Institute of Technology,2017,49(6):150–155.[曾加东,李明水,李少鹏.矩形高层建筑顺风向脉动风荷载空间相关性[J].哈尔滨工业大学学报,2017,49(6):150–155.]

[7] Yuan Jiahui,Chen Shuifu,Xia Yuchao,et al.Spatial correlation of along-wind fluctuating wind loads on rectangular high-rise buildings[J/OL].Journal of Beijing University of Aeronautics and Astronautics,1–13.[2025–09–28].https://doi.org/10.13700/j.bh.1001-5965.2023.0828.[袁家辉,陈水福,夏俞超,等.矩形高层建筑顺风向脉动风荷载空间相关性[J/OL].北京航空航天大学学报,1–13.[2025–09–28].https://doi.org/10.13700/j.bh.1001-5965.2023.0828.]

[8] Vickery B J,Clark A W.Lift or across-wind response of tapered stacks[J]. Journal of the Structural Division, 1972, 98 (1):1–20.

[9] Liang Shuguo, Liu Shengchun, Li Q S, et al. Mathematical model of acrosswind dynamic loads on rectangular tall buildings[J].Journal of Wind Engineering and Industrial Aerodynamics,2002,90(12/13/14/15):1757–1770.

[10] Gu Ming, Tang Yi, Quan Yong. Fluctuating force or torsional acting on rectangular super-tall buildings: Part I: Basic characteristics[J]. Journal of Vibration and Shock, 2010, 29(6): 42–45.[顾明,唐意,全涌.矩形超高层建筑横风向脉动风力,I:基本特征[J].振动与冲击,2010,29(6):42–45.]

[11] Tang Yi, Gu Ming, Quan Yong. Fluctuating force of torsional acting on rectangular super-tall buildings: Part Ⅱ: Mathematical model[J].Journal of Vibration and Shock,2010,29(6):46–49.[唐意,顾明,全涌.矩形超高层建筑横风向脉动风力,Ⅱ:数学模型[J].振动与冲击,2010,29(6):46–49.]

[12] Wei Qike, Li Zhengliang, Huang Hanjie, et al. Fluctuating pressure correlativity test analysis on super-tall buildings[J]. Journal of Experiments in Fluid Mechanics,2010,24(5):63–69.[魏奇科,李正良,黄汉杰,等.超高层建筑表面脉动风压空间相关特性试验研究[J].实验流体力学,2010,24(5):63–69.]

[13] Liang Shuguo, Li Q S, Liu Shengchun, et al. Torsional dynamic wind loads on rectangular tall buildings[J]. Engineering Structures,2004,26(1):129–137.

[14] Gu Ming, Tang Yi, Quan Yong. Basic characteristics of torsional fluctuating wind force on rectangular super-tall buildings[J].Journal of Building Structures,2009,30(5):191–197.[顾明,唐意,全涌.矩形截面超高层建筑风致脉动扭矩的基本特征[J].建筑结构学报,2009,30(5):191–197.]

[15] Tang Yi, Gu Ming, Quan Yong. Mathematical model of torsional fluctuating wind force on rectangular super-tall buildings[J]. Journal of Building Structures, 2009, 30(5): 198–204.[唐意,顾明,全涌.矩形截面超高层建筑风致脉动扭矩的数学模型[J].建筑结构学报,2009,30(5):198–204.]

[16] Huang Dongmei,Zhu Ledong.Mathematical model of spatial correlation of wind pressure coefficients for super-tall buildings:Comprehensive analysis method[J].China Civil Engineering Journal,2009,42(8):26–36.[黄东梅,朱乐东.超高层建筑层风力空间相关性数学模型——综合分析法[J].土木工程学报,2009,42(8):26–36.]

[17] Huang Dongmei, Zhu Ledong. Study on spatial correlation functions of wind loads on a super-tall building—Analysis and induction method[J].China Civil Engineering Journal,2010,43(9):32–39.[黄东梅,朱乐东.超高层建筑层风力空间相干函数研究——分析归纳法[J].土木工程学报,2010,43(9):32–39.]

[18] Huang D M, Zhu L D, Chen W, et al. Vertical coherence functions of wind forces and influences on wind-induced responses of a high-rise building with section varying along height[J].Wind and Structures,2015,21(2):119–158.

[19] Ho T C E,Surry D,Morrish D,et al.The UWO contribution to the NIST aerodynamic database for wind loads on low buildings: Part I: Archiving format and basic aerodynamic data[J]. Journal of Wind Engineering and Industrial Aerodynamics,2005,93(1):1–30.

[20] ESDU. Characteristics of atmospheric turbulence near the ground: Part II: Single point data for strong winds(neutral atmosphere): ESDU—85020[S]. London: Engineering Sciences Data Unit,1985.

[21] ESDU. Strong winds in the atmospheric boundary layer: Part I: Hourly-mean wind speeds: ESDU—82026[S]. London:Engineering Sciences Data Unit,1982.

[22] ESDU. Characteristics of atmospheric turbulence near the ground: Part II: Single point data for strong winds(neutral atmosphere): ESDU—74031[S]. London: Engineering Sciences Data Unit,1974.

[23] Hunt A. Wind-tunnel measurements of surface pressures on cubic building models at several scales[J]. Journal of Wind Engineering and Industrial Aerodynamics, 1982, 10(2):137–163.

[24] Yuan Jiahui, Chen Shuifu, Liu Yi. Characteristics of torsional force of rectangular high-rise buildings with different side ratios[J].Journal of Central South University(Science and Technology),2021,52(12):4361–4371.[袁家辉,陈水福,刘奕.不

同长宽比矩形高层建筑的横风向风力特性[J].中南大学学报(自然科学版),2021,52(12):4365–4371.]

[25] Yuan Jiahui, Chen Shuifu, Liu Yi. Aerodynamic base moment coefficients of rectangular high-rise buildings[J]. Journal of Harbin Institute of Technology,2023,55(9):54–62.[袁家辉,陈水福,刘奕.矩形高层建筑气动基底力矩系数研究[J].哈尔滨工业大学学报,2023,55(9):54–62.]

[26] Yuan Jiahui,Chen Shuifu,Liu Yi.Non–Gaussian features of fluctuating wind pressures on rectangular tall buildings with large side ratio[J].Journal of Harbin Institute of Technology,2025,57(1):46–55.[袁家辉,陈水福,刘奕.大深宽比矩形高层建筑表面脉动风压非高斯特性[J].哈尔滨工业大学学报,2025,57(1):46–55.]

[27] Lin Ning,Letchford C,Tamura Y,et al.Characteristics of wind forces acting on tall buildings[J].Journal of Wind Engineering and Industrial Aerodynamics,2005,93(3):217–242.

Spatial Correlation of Torsional Fluctuating Wind Loads on Rectangular High-rise Buildings

YUAN Jiahui[1,2], *CHEN Shuifu*[2*], *XIA Yuchao*[3], *LIU Yi*[2]

(1.WISDRI City Construction Engineering & Research Incorporation Limited, Wuhan 430063, China;
2.College of Civil Engineering and Architecture, Zhejiang University, Hangzhou 310058, China;
3.Zhejiang Southeast Space Frame Company Limited, Hangzhou 311209, China)

Abstract:

Objective Tall buildings in contemporary construction practice predominantly adopt slab-type designs with substantial side ratios. In these rectangular tall structures, the response to torsional wind vibrations becomes a critical issue. Accurate calculation of wind-induced vibrations requires a comprehensive understanding of the spatial correlation of fluctuating wind loads. Existing torsional coherence function models, derived from wind tunnel tests on specialized or small side ratio building models, often neglect the effect of diverse building section forms on the coherence function. Therefore, their applicability to common tall buildings with larger side ratios remains limited. This study addresses this limitation by proposing a series of spatial correlation mathematical models for torsional fluctuating wind loads on high-rise buildings, enhancing their practicality and applicability.

Methods Firstly, four types of wind fields (O1, S1, O2, and S2) were simulated based on data from the Engineering Sciences Data Unit (ESDU). The mean wind speed profile was generated using the logarithmic rate formula recommended by ESDU—85020. The theoretical turbulence intensity profile was produced based on the formula recommended by ESDU—82026. The turbulence integral scale was determined using the formula indicated by ESDU—74031, and the fluctuating wind speed spectrum was obtained using the von–Karman spectrum recommended by ESDU—74031. Turbulence intensity in S–type wind fields was greater than that in O–type wind fields, and the turbulence integral scale in type–1 wind fields was larger than that in type–2 wind fields. Secondly, 21 test models with side ratios ranging from 1/9.0 to 9.0 were created by assembling 12 segments, using a length scale of 1∶200. The completed model measured 0.50 m in height, 0.06 m in width, and 0.06 to 0.54 m in length. Seven layers of measuring points were placed vertically at heights of 0.10*H*, 0.30*H*, 0.50*H*, 0.65*H*, 0.80*H*, 0.90*H*, and 0.98*H*. The measuring point layers were numbered 1 to 7 from bottom to top, maintaining a consistent arrangement across all layers. Finally, synchronous pressure measurement wind tunnel tests were conducted on the 21 models under four wind fields. Time history data of wind pressure coefficients at the measuring points on the models were collected using synchronous pressure scanning valves. The sampling frequency was 400 Hz, and the sampling duration was 90 s, producing a total of 36 000 data points.

Results and Discussions Based on the experimental results, the vertical correlation coefficient and coherence function of buildings with various side ratios under different wind fields were calculated. The influences of side ratio, turbulence intensity, and turbulence integral scale on the vertical correlation coefficient and coherence function of torsional fluctuating wind loads were analyzed. Mathematical models of the vertical spatial correlation of torsional fluctuating wind loads for rectangular high-rise buildings with side ratios ranging from 1/9.0 to 9.0 were established using the least squares method, and the accuracy of these models was compared to the experimental data. The results showed that the correlation coefficient of torsional fluctuating wind load exponentially decreased with increasing separation distance, and the attenuation rate varied with side ratio. When $D/B \leq 1.0$, the correlation coefficient of torsional fluctuating wind load remained greater than 0, and the attenuation rate of the correlation coefficient increased with a higher side ratio. When $D/B > 1.0$, the correlation coefficient of torsional fluctuating wind load became highly discontinuous, and the attenuation rate of the correlation coefficient decreased with a higher side ratio. For some buildings, the correlation coefficient even became negative at positions with large separation distances between measuring point layers. When $D/B < 1.0$, the correlation coefficient of torsional fluctuating wind load was only slightly affected by the turbulence characteristics of

the incoming flow, whereas when $D/B \geq 1.0$, the correlation coefficient became negative at large separation distances due to changes in turbulence characteristics. The initial value of the torsional fluctuating coherence function was influenced by the side ratio and the separation distance of the building. For buildings with $1/5.0 \leq D/B \leq 5.0$, the spectral peak of the coherence function was evident. When $D/B \leq 1.0$, the corresponding reduced frequency was slightly greater than 0.1, consistent with the Strouhal number, indicating that the spectral peak was generated by vortex shedding. When $D/B > 1.0$, the corresponding reduced frequency of the spectral peak gradually decreased. The coherence function of buildings with various side ratios changed with frequency. When $D/B \leq 1.0$, the coherence function initially decreased, then increased, and finally dropped rapidly to a low coherence level. When $1.0 < D/B \leq 5.0$, the coherence function for large separation distances decreased slowly with frequency, while for small separation distances, it fluctuated repeatedly at a low coherence level. When $D/B > 5.0$, the coherence function quickly decayed with frequency and then fluctuated at a low coherence level. The coherence function of torsional wind load exhibited complexity, being affected by both separation distance and mean velocity. Across different wind fields, the coherence function displayed significant fluctuations with frequency and building side ratio.

Conclusions The proposed correlation coefficients and coherence functions for torsional fluctuating wind loads on rectangular tall buildings show strong consistency with experimental observations. These results carry important implications for structural design and load code revisions, providing critical insights for reducing wind-induced vibrations in tall buildings.

Key words: rectangular high-rise building; torsional fluctuating wind load; spatial correlation; wind tunnel test; side ratio; mathematical model

（编辑　周　璇）

引用格式: Yuan Jiahui,Chen Shuifu,Xia Yuchao,et al.Spatial correlation of torsional fluctuating wind loads on rectangular high-rise buildings[J].Advanced Engineering Sciences,2025,57(6):178–190.[袁家辉,陈水福,夏俞超,等.矩形高层建筑扭转向脉动风荷载空间相关性[J].工程科学与技术,2025,57(6):178–190.]